Applied Surface Science 497 (2019) 143815

Contents lists available at ScienceDirect

Applied Surface Science

journal homepage: www.elsevier.com/locate/apsusc

Full length article

Adsorption of hydrogen sulfide by amine-functionalized metal organic framework (MOF-199): An experimental and simulation study☆

Hong-Yan Zhang[a], Chao Yang[a], Qiang Geng[a], Hui-Ling Fan[a,*], Bao-Jun Wang[a,*], Meng-Meng Wu[a], Zhen Tian[b]

[a] State Key Laboratory of Coal Science and Technology, Co-founded by Shanxi Province and the Ministry of Science and Technology, Institute for Chemical Engineering of Coal, Taiyuan University of Technology, West Yingze Street Number 79, Taiyuan 030024, PR China
[b] Department of Analysis, Service Center Micromertics Instrumental Ltd., Shanghai 200000, PR China

ARTICLE INFO

Keywords:
Metal-organic framework (MOF-199)
Amine-functionalized
Sulfur adsorption
DFT calculations

ABSTRACT

A series of amine modified MOF-199 adsorbents were prepared by impregnation method for using H_2S room temperature removal. The parent and functionalized materials were characterized by XRD, FT-IR, SEM, N_2 adsorption/desorption isotherms, and XPS. It was indicated that the structure of MOF-199 can be maintained after modification by appropriate tertiary amine triethanolamine (TEA), while primary amine monoethanolamine (MEA) and secondary amine diethanolamine (DEA) modification can destroy its structure due to the strong interaction with MOF-199. Breakthrough results showed that MOF-199 functionalized by TEA presented an improved H_2S adsorption capacity of 2.74 mmol/g, higher than that of parent MOF-199 (1.67 mmol/g). Whereas, grafting of MEA and DEA into MOF-199 led to the sulfur capacity decrease to 0.83 mmol/g and 0.58 mmol/g, respectively. Calculation by density functional theory revealed that the binding energies of H_2S adsorption on the TEA/MOF-199 were larger than that on bare MOF-199, which was considered to contribute to the improved adsorption. The enhanced binding energy of H_2S on the TEA/MOF-199 was attributed to the hydroxyl in TEA.

1. Introduction

Natural gas is widely used in civil combustion, power generation, chemical industry and other fields [1]. Capturing hydrogen sulfide (H_2S) from nature gas is indispensable due to its high corrosion and toxicity [2]. To remove H_2S, different techniques have been studied including amine scrubbing desulfurization [3], biological desulfurization [4] and adsorption desulfurization and so on. Currently, adsorption desulfurization using porous materials is deemed to be an attractive method due to its easy operation, low cost and high desulfurization precision [5]. An excellent category of such materials is the metal−organic frameworks (MOFs) made up of organic linkers bonded with metal ions to form multiaperture framework structure that has the advantages of high surface area and porosity, easily designed and functionalized pore structure [6–8]. This materials present great potential for gas separation, adsorption, storage, or as catalysis [9–14].

In recent years, a large number of MOFs have been synthesized and researched for removing sulfur compounds [15–18]. For examples, Li et al. [19] investigated five typical MOFs (i.e., HKUST-1, MIL-101(Cr), MIL-53(Fe, Cr), and MOF-5(Zn)) using for aromatic sulfur compounds removal. They demonstrated that the adsorbate−adsorbent interaction was the most important factor affecting adsorption performance. Brieva et al. [20] reported that MOF-199 has a high sulfur uptake capacity because of the stronger interaction between the Cu^{2+} ions and the S-atom of DBT. Achmann et al. [21] revealed that the smaller pores in MOF-199 provided a better stabilization of the small molecular sulfur compound by Van-der-Waals force that made MOF-199 presented a significant potential for sulfur removal from gasoline or diesel fuel. Hamon et al. [22] concluded that the hydrogen bond was main interaction between H_2S molecules and MIL-47(V) as well as MIL-53(Cr). In addition, the study of MOFs on adsorptive removal of sulfur compounds also included MOF-74 (with coordinatively unsaturated sites) [23], UIO-66(Zr) (with a high structure stability) [24,25], and IRMOF-3 (with functional-amino group) [26]. However, all the MOFs mentioned above fail to meet the requirements of industrial desulfurization because of the low capacities.

Recently, many modification methods have been reported to improve the adsorption performance of MOFs. Novel functional groups

☆ Full length article

* Corresponding authors.
E-mail address: fanhuiling@tyut.edu.cn (H.-L. Fan).

https://doi.org/10.1016/j.apsusc.2019.143815
Received 12 June 2019; Received in revised form 21 August 2019; Accepted 26 August 2019
Available online 27 August 2019
0169-4332/

can be facilely introduced into the as-synthesized MOF structure through postsynthetic modification [27–29]. From a mechanistic standpoint, the amino is beneficial for H_2S adsorption. There are two main methods to acquire amino-functionalized MOF materials [30]. On the one hand, introducing amino groups into ligands can obtain the amino-tagged MOF structures [31–34]. However, aromatic amino-tagged MOFs often exhibit slow adsorption kinetics [35]. On the other hand, amine reagents directly grafting on the metal centers of MOFs has been investigated as a highly effective technique for toxic molecules adsorption [36–39]. Su et al. [40] researched the postsynthetic Mg-MOF-74 with tetraethylenepentamine (TEPA) and tested for CO_2 removal under dry and humid conditions. They found that TEPA interacted preferentially with the open-metal sites situated on the surface of MOF-74. The adsorption capacity of the TEPA-MOF for CO_2 was about 15% higher than that of the original MOF because of the extra adsorption sites supplied by the multiunit amines. Peng and co-workers [41] investigated a modified MOF-808 by EDTA which showed a high removal efficiency of > 99% in metal ion capture. The excellent performance can be traceable to the strong chelation between metal ions and EDTA in the well-dispersed ordered structure of MOF-808-EDTA. Li et al. [42] found that triethylenediamine (TED) and hexamethylenetetramine (HMTA) functionalized MIL-101(Cr) exhibited a high CH_3I saturation uptake capacity. This can be attributed to the effective grafting of TED and HMTA onto the MOF pore surface, which created molecular traps that offered greatly enhanced bonding interactions toward organic iodides. It can be seen that the extra binding site provided by the amines is the main reason for MOFs having a good performance to toxic molecules.

Amine scrubbing is a commonly used technology for removing H_2S from various gas streams in industry, as the amine solution has a higher capacity for removing acidic gases [3]. This inspires us to graft MOFs with amines and expected to increase H_2S adsorption.

This paper reports grafting MOFs with different amine at the appropriate amounts and the evaluation results of dynamic breakthrough test. The candidate amine include primary amine monoethanolamine (MEA), secondary amine diethanolamine (DEA) and tertiary amine triethanolamine (TEA). Several different characterization methods containing Fourier transform infrared (FT-IR), X-ray diffraction (XRD), scanning electron microscopy (SEM), N_2 adsorption/desorption isotherms, and X-ray photoelectron spectroscopy (XPS) are used to analyze the parent and functionalized materials. The DFT calculations give the graft models of TEA in the MOF-199 and the interactions between H_2S and TEA/MOF-199 materials.

2. Experimental preparation

2.1. Sample preparation

$Cu(NO_3)_2{\cdot}3H_2O$ (AR, 99%), *N*,*N*-dimethyflormamide (DMF) (AR, 99%), dichloromethane (AR, 99.9%) and Ethanol (AR, 99%) were produced from Kermel Chemical Reagent Co. Ltd. 1,3,5-benzenetricarboxylic acid (BTC) (AR, 98%), MEA (AR, 99%), DEA (AR, 99%), and TEA (AR, 98%) were produced from Aladdin Chemical Co. Ltd. All the raw materials used in this paper did not do any further purification.

MOF-199 was synthesized according to literature methods [43,44]. The synthesis processes were as below: $Cu(NO_3)_2{\cdot}3H_2O$ (2 g) and BTC (1 g) were respectively dissolved in deionized water (17 mL) and a mixture of ethanol (17 mL) with DMF (17 mL). The solution was stirred evenly and then poured in a 100 mL teflon reactor, capped, keeping at 85 °C for 24 h. Pouring out the supernatant obtained the blue crystals, which was filtered and washed with DMF and ethanol, and the solvent was exchanged with dichloromethane every day, for a total of 2–3 washes. After filtered, the powder was then dried at 45 °C overnight and then activated at 180 °C for 24 h under N_2 flow. The resulting product was kept in a desiccator for amine functionalization using.

The amine-functionalized MOF-199 was prepared by wetness impregnation using 0.300 g of activated MOF-199 adding to a certain amount of amine in a solution containing 10 mL of methanol. Then the mixture was stirred in a 100 ml beaker for 12 h. A blue precipitate was obtained by filtration and washed with methanol for several times to remove unreacted amine. Subsequently, the solid sample was dried at 60 °C for 12 h. Before evaluating samples, the samples were activated at 120 °C for 12 h. The amount of the impregnated amine is added in accordance with the molar ratio of the nitrogen in the amine compounds to the copper in the MOF-199, and the molar ratio is expressed by n. The modified materials are referred to as amine/MOF-199-n with n = 1, 2, and 3.

2.2. Characterization of materials

The powder X-ray diffraction (XRD) patterns were measured on RigakuD/max-2500 diffractometer, using CuKα radiation (λ = 1.541 Å). The data were recorded from 5° to 50° (2θ). Nicolet Magna-IR830 spectrometer was chosen to obtain the Fourier transform infrared (FTIR) spectra dates. KBr was used as the background at the same conditions. N_2 adsorption/desorption isotherms using a MicroActive for ASAP 2460 instrument were measured at a relative pressure(P_{N2}/P_0) range of 0.002–0.99 and then employed to determine surface area with Brunauer-Emmett-Teller (BET) method, pore volume with t-plot method. X-ray photoelectron spectrometer (XPS) was used to analyze the surface electronics of the materials. It was acquired with an Thermo Scientific Escalab 250Xi Spectrometer with Al K radiation. Scanning electron microscopy (SEM) images were taken by MERLIN compact-61-78 instrument. Thermogravimetric (TG) curves were measured by Setaram SETSYS Evolution TGA instrument. The temperature was increased from 30 to 700 °C at a rate of 10 °C/min. The carrier gas was nitrogen with a rate of 100 mL/min. If it has no especial illustration, the characterization materials were MEA/MOF-199-2, DEA/MOF-199-2 and TEA/MOF-199-2.

2.3. Desulfurization measurements

The H_2S breakthrough capacity of materials was evaluated in a fixed-bed reactor. The reactor was a quartz U-tube with inner diameter of 6 mm. The inlet concentration of H_2S was 600 mg/m^3, which diluted with nitrogen in high purity, and the total inlet flow rate was 100 mL/min. When the outlet gas concentration is 1% of the import gas concentration, it is regarded as bed breakthrough. The breakthrough sulfur capacity was defined as xx mmol of H_2S removed per gram of adsorbent (mmol/g).

2.4. Simulation models

MOF-199 is assembled from copper ions and BTC ligands to form the “cage-channel” structure, including 9 × 9 Å channel and 5 Å pore cages, show in Fig.1a [45–47]. The two types of pore are connected by the copper dimer configurations, which are the most important adsorption sites of MOF-199 [48]. And the coordination orientation of unsaturated copper dimer with the small molecule faces the square-shaped channel. Therefore, we intercept square-shaped channel (as shown in Fig.1b) to simulate the way of MOF-199 loading amine compounds and the adsorption of H_2S on amine functionalized MOF-199.

2.5. Computational method

Theoretical investigation was carried out using density functional theory (DFT) calculations with DMol^3 [49] module in the Accelrys software package Materials Studio. The generalized gradient approximation (GGA) [50] correlation functional of Perdew-Burke-Ernzerhof (PBE) parametrization with the double numerical plus (DNP) polarization basis set was employed. The Density functional semi-core

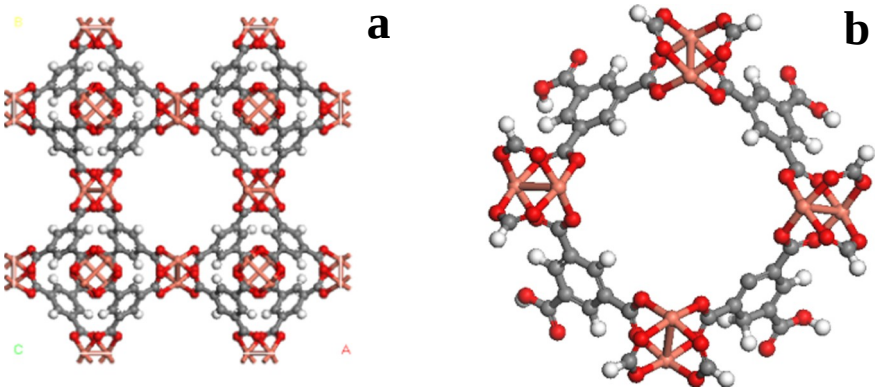

Fig. 1. (a) Topological structure of MOF-199, (b) computational model (the gray is C, the red is O, the white is H, and the pink is Cu).

pseudopotentials (DSPP) [51] fitted to all electron relativistic DFT results and areal-space orbital global cutoff of 4.4 Å was applied. The dispersion corrected DFT (DFT-D) scheme was introduced to describe the van der Waals (vdW) interaction.

The binding energies (BEs) for the MOF-199 with amine are defined as $E_b = -(E_{MOF\text{-}199\text{-}amine} - E_{MOF\text{-}199} - mE_{amine})/m$, where $E_{MOF\text{-}199\text{-}amine}$ is the total energy of amine grafted MOF-199, $E_{MOF\text{-}199}$ and E_{amine} are the total energies of an isolated MOF-199 and a amine molecule, respectively, and m is the number of amine molecule. Similarly, the average adsorption energy (AE) for H_2S is defined as $Ea = -(E_{MOF\text{-}199\text{-}amine\text{-}nH2S} - E_{MOF\text{-}199\text{-}amine} - nE_{H2S})/n$, where $E_{MOF\text{-}199\text{-}amine\text{-}nH2S}$ is the total energies of nH_2S adsorbed on the MOF-199-amine, E_{H2S} is the total energies of an isolated H_2S.

3. Results and discussion

3.1. Characteristics of the adsorbents

The modification results of MOF-199 by amines are evidenced by the FTIR spectra (Fig. 2). For MOF-199, there are several typical adsorption bands, such as the bands at 1372, 1446 cm^{-1} and 1644 cm^{-1}, which are attributed to the symmetric and asymmetric vibrations of the carboxylate groups [52]. Besides that, several peaks in region of 1300–700 cm^{-1} belonging to the out-of-plane vibrations of benzene are observed [53]. These bands can also be found in all amine modified MOFs. For MEA/MOF-199 and DEA/MOF-199, the broad band in the range of 3250–3310 cm^{-1} with horseshoe-shaped peak and adsorption bond at 3243 cm^{-1} with a single peak can be assigned to the asymmetric and symmetric $-NH_2$ and $-NH$ vibrations, respectively, which are not presented in parent MOF-199. In addition, the band located at ~1050 cm^{-1} assigning to the C—N stretching vibration of alkylamines [54], can be found in series of amine modified MOF-199. The above results clearly demonstrated that the amine-functionalized MOF-199 has been successfully prepared.

Fig.3 presents the XRD patterns of prepared MOFs. The results show that the characteristic peaks of MOF-199 remain unchanged when TEA is grafted into MOF-199, indicating that the crystal structure of sample remains intact after TEA modification. However, these diffraction peaks are greatly changed after grafting MEA and DEA, suggesting a serious structure change. In addition, an obvious change about the XRD patterns of MOF-199 can be found even adding a little amount of MEA and DEA.

The surface topography of the parent and amine-functionalized MOF-199 materials were characterized using SEM characterization. As seen in Fig. 4a and b, TEA/MOF-199 shows pyramidal in morphology and very similar to the parent MOF-199, although some irregular small crystals were also observed in TEA/MOF-199 samples. For MEA/MOF-199 and DEA/MOF-199, significant shape changes are observed (Fig. 4c and d. They gave the SEM images of “a collapsed tall building”. These results illustrate that grafting of MEA and DEA into MOF-199 leads to a destruction of the structure of MOF-199, as revealed by XRD characterization. The different behavior originates from the different interaction between amine and MOFs. The -NH group of MEA and DEA can easily attach to the copper center and take place strong interactions, thus destroys the MOF-199 structure. However, since the TEA molecule is large, and the steric hindrance inhabits a strong interaction with MOF-199, and maintains the structure.

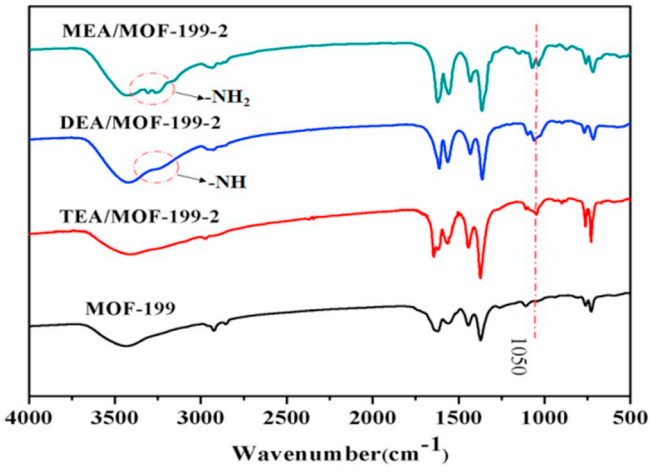

Fig. 2. FT-IR spectrum for MOF-199 and the modified materials.

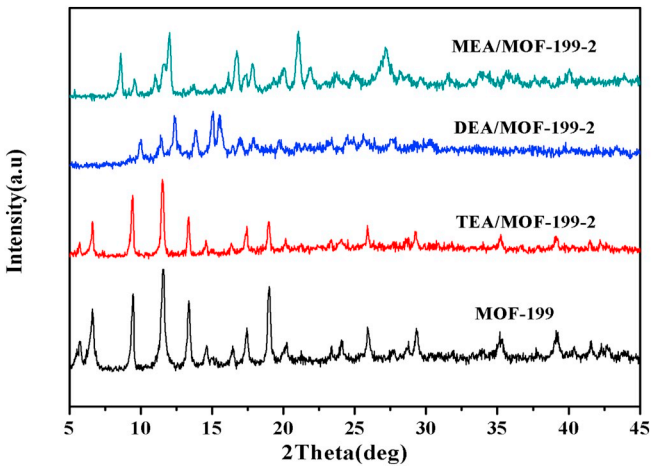

Fig. 3. Powder X-ray diffraction spectrum of MOF-199 and the modified materials.

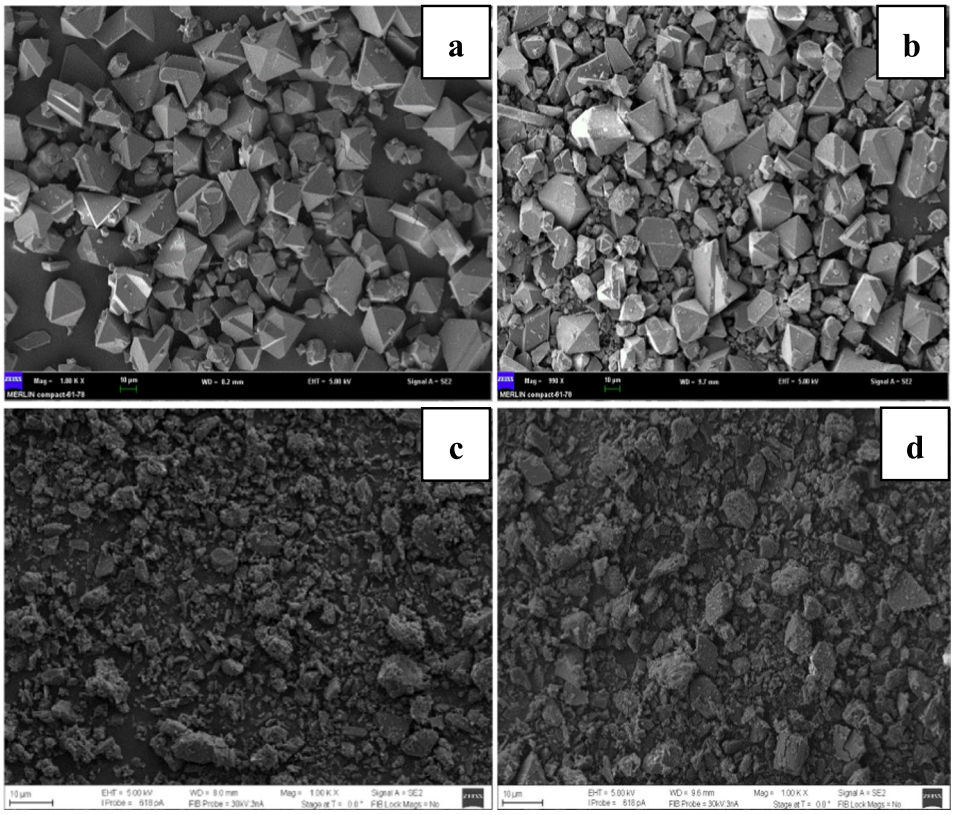

Fig. 4. SEM images of (a) MOF-199, (b) TEA/MOF-199-2, (c) DEA/MOF-199-2, and (d) MEA/MOF-199-2.

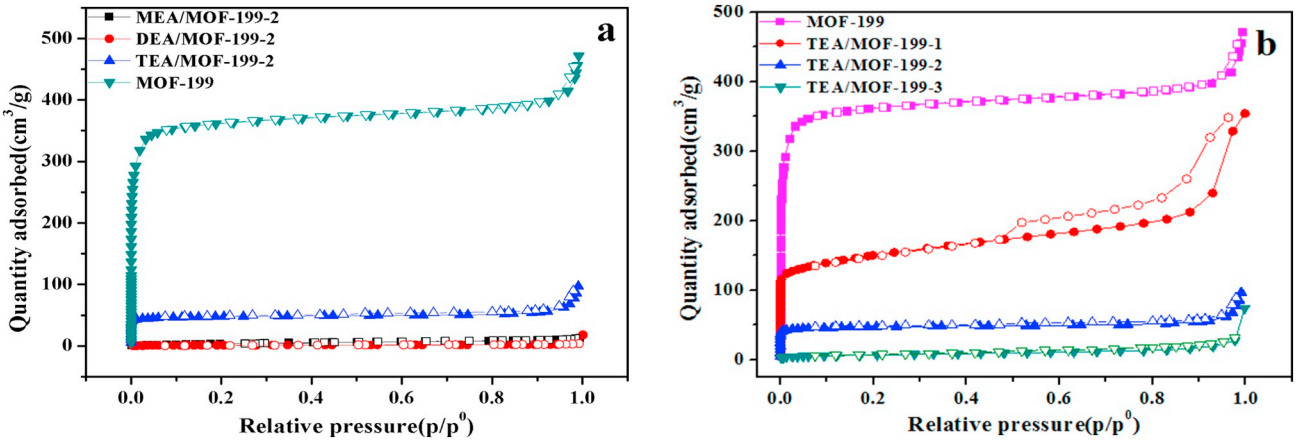

Fig. 5. Nitrogen adsorption – desorption isotherms of samples at 77 K.

Table 1
Textural parameter of MOF-199 and modified materials.

Samples	S_{BET}(m^2/g)	V_t(cm^3/g)	V_{mic}(cm^3/g)	Pore diameter(nm)
MOF-199	1459	0.73	0.55	0.52
TEA/MOF-199-2	187	0.15	0.07	0.43
DEA/MOF-199-2	4	0.01	0.001	1.16
MEA/MOF-199-2	18	0.02	0.01	1.28

Table 2
Textural parameter of MOF-199 and TEA/MOF-199 materials.

Samples	S_{BET}(m^2/g)	V_t(cm^3/g)	V_{mic}(cm^3/g)	Pore diameter(nm)
MOF-199	1459	0.73	0.55	0.52
TEA/MOF-199-1	550	0.55	0.21	0.43
TEA/MOF-199-2	187	0.15	0.07	0.42
TEA/MOF-199-3	25	0.12	0.01	0.75

The parameters of surface area and porous structure were measured by N_2 adsorption–desorption isotherms, as shown in Fig. 5a and Table 1. Compared with MOF-199, the grafted materials exhibit a rapid reduction in both specific surface areas and pore volumes, consistent with the results in the references [38, 41, 42]. Specifically, the surface area decreases obviously from 1459 m^2/g^{-1} for pristine MOF-199 to 186 m^2/g^{-1} for TEA/MOF-199, 4 m^2/g^{-1} for DEA/MOF-199 and 18 m^2/g^{-1} for MEA/MOF-199, and pore volumes decreased from 0.73 cm^3/g^{-1} to 0.15 cm^3/g^{-1}, 0.01 cm^3/g^{-1} and 0.02 cm^3/g^{-1}, respectively. Compare to bare MOF-199, the TEA-grafted materials showed a reduced pore diameters from original 0.52 nm [55]. The decreased pore diameters are thought to be induced by filling pores.

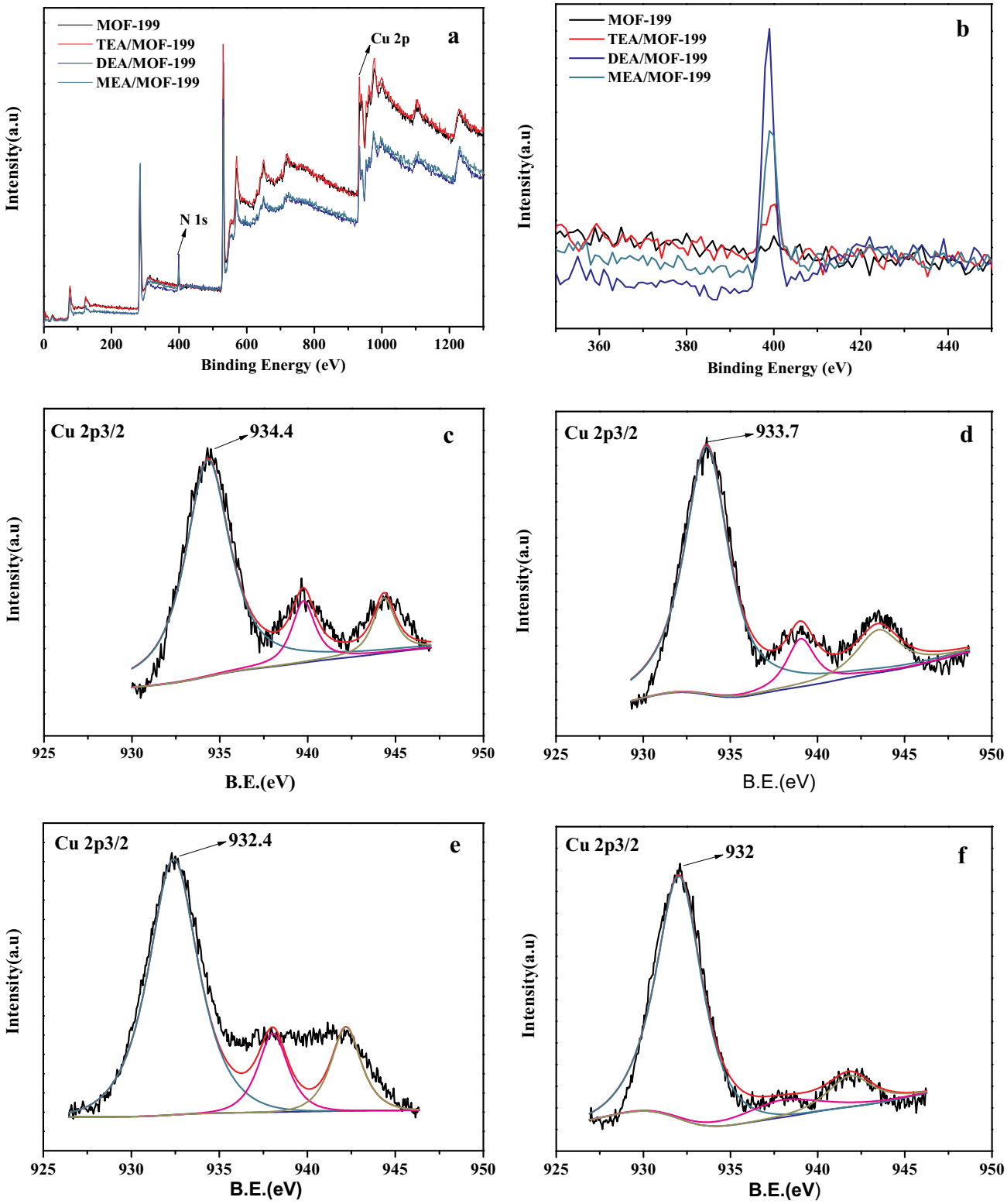

Fig. 6. XPS spectra of (a) various modified MOFs, (b) High-resolution N 1s scan and the Cu 2p3/2 for (c) MOF-199, (d) TEA/MOF-199-2, (e) DEA/MOF-199-2, (f) MEA/MOF-199-2.

Whereas, DEA/MOF-199 and MEA/MOF-199 exhibit increased pore diameters to 1.16 and 1.28 nm, which is considered to be caused by the collapse of MOF-199 structure.

Fig. 5b exhibits the adsorption–desorption isotherms of N_2 on MOF-199 and modified MOF-199 by different amount of TEA at 77 K. It indicates that the adsorption amount of N_2 on TEA/MOF-199 s are much lower than that of the original MOF-199, and become gradually low with the increase of TEA loading. However, the pore diameters reduce from 0.52 nm to 0.43 nm, 0.42 nm, but increase to 0.75 nm (See Table 2), suggesting a destruction of structure occurred after excessively loading of TEA.

Fig.6 presents the XPS survey spectra, high resolution N 1 s region

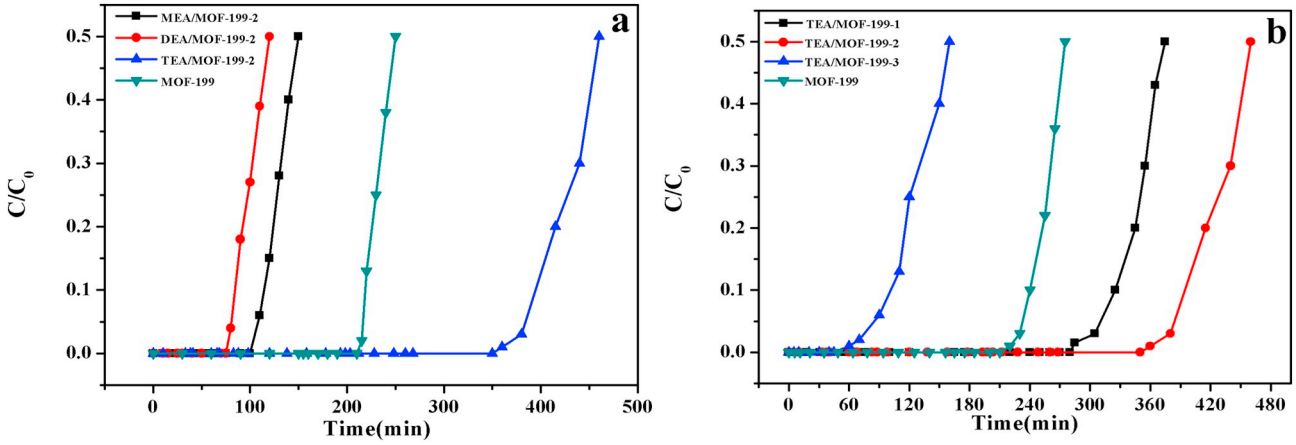

Fig. 7. H_2S removal breakthrough curves measured on the materials.

Table 3
H_2S breakthrough capacities for the samples studied.

Samples	Average adsorption capacities (mmol/g)	STD
MOF-199	1.67	0.29
MEA/MOF-199-2	0.83	0.10
DEA/MOF-199-2	0.58	1.09
TEA/MOF-199-1	2.14	0.73
TEA/MOF-199-2	2.74	0.20
TEA/MOF-199-3	0.33	0.61

and Cu $2p_{3/2}$ region for MOF-199 and amine modified MOF-199. As seen from Fig. 6b, the amine functionalized MOF-199 shows the intense peak for N 1 s, which is absent from parent MOF-199. From Fig. 6c, the intense peak for Cu $2p_{3/2}$ located at a binding energy (BE) of 934.4 eV is attributed to a characteristic value for Cu—O in MOF-199 [18,56]. The next two peaks are satellite peaks of copper. The high-resolution Cu $2p_{3/2}$ scans, shown in Fig. 6d, e and f, present a shift to lower binding energy for the amine functionalized MOF-199 (~934.4 eV for MOF-199 vs. 933.7 eV for TEA/MOF-199, 932.4 eV for DEA/MOF-199 and 932 eV for MEA/MOF-199). Cu-atom changes into more electronegative suggests receiving the electrons from the donor of oxygen or nitrogen atoms in alcoholamine compound. In addition, DEA/MOF-199 and MEA/MOF-199 have a more shift of binding energy than that of TEA/MOF-199, indicating the stronger interactions for DEA and MEA molecules with copper ions. This is in consistent with the results from XRD, N_2 adsorption－desorption mentioned above.

3.2. Desulfurization performance

The removal performance of H_2S on the prepared samples was evaluated at 30 °C in a fixed-bed reactor. The obtained breakthrough curves are shown in Fig. 7. In order to ensure the reliability of the experimental data, the adsorption capacity on each sample is the average result of three experiments. The average sulfur capacity of each sample and its standard deviation are listed in Table 3.

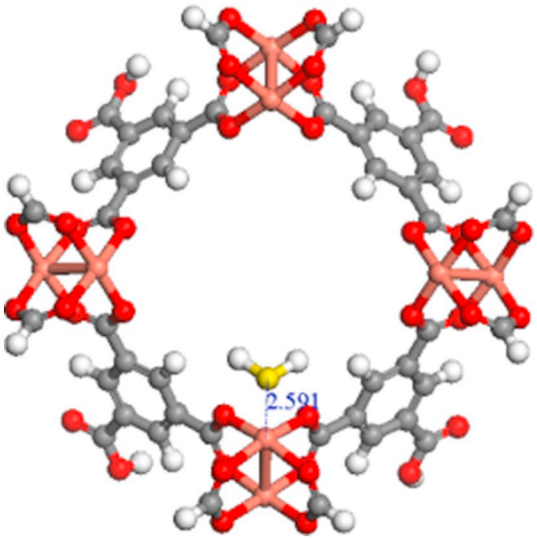

Fig. 9. The models of H_2S molecule adsorption on the MOF-199.

As show in Fig. 8a and Table 3, MOF-199 can efficiently remove H_2S with a breakthrough capacity of 1.67 mmol/g. However, both the MEA and DEA modified samples show a poor performance than that of the bare MOF-199. The bad desulfurization performances of MEA/MOF-199 and DEA/MOF-199 are believed to relate to the collapse of the MOFs structure, revealing in XRD, SEM and N_2 adsorption characterizations. Actually, some other primary and secondary amine compounds, including polyethylene imide, tetraethylene pentamine,

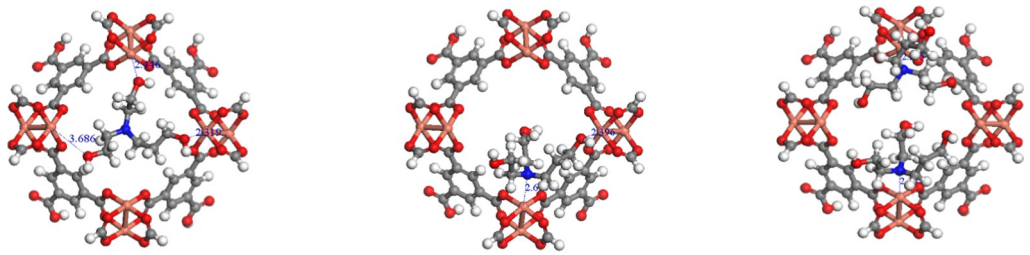

（a）E_b=153.5 kJ/mol (P-1)　（b）E_b =139.9 kJ/mol (V-1)　（c）E_b =119.2 kJ/mol(V-2)

Fig. 8. The models of TEA loading into MOF-199.

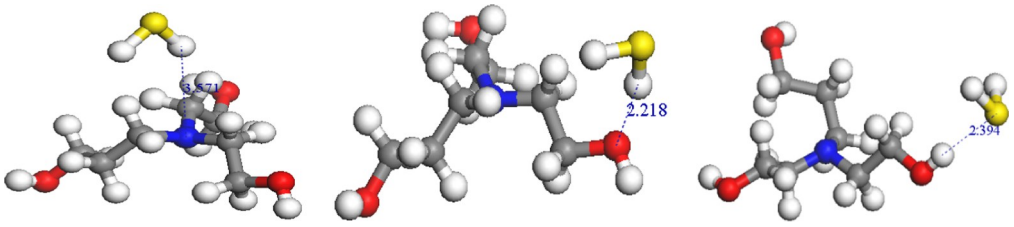

（a）E_a=8.70 kJ/mol （b）E_a=17.74 kJ/mol （c）E_a=19.72 kJ/mol

Fig. 10. The models of H_2S molecule adsorption on the TEA.

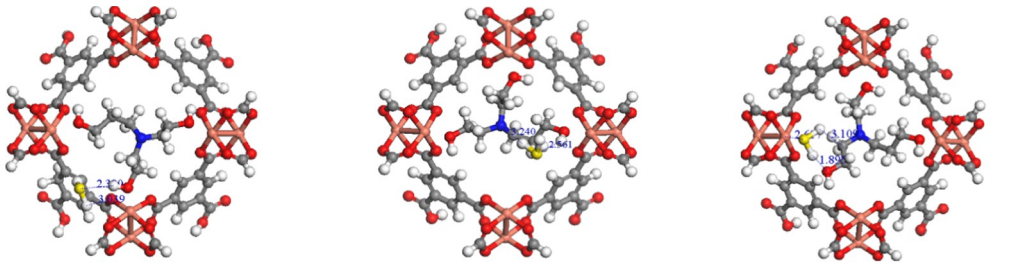

（a）E_a=87.1 kJ/mol(P-1) （b）E_a=87.3 kJ/mol(P-1) （c）E_a=92.1 kJ/mol(P-1)

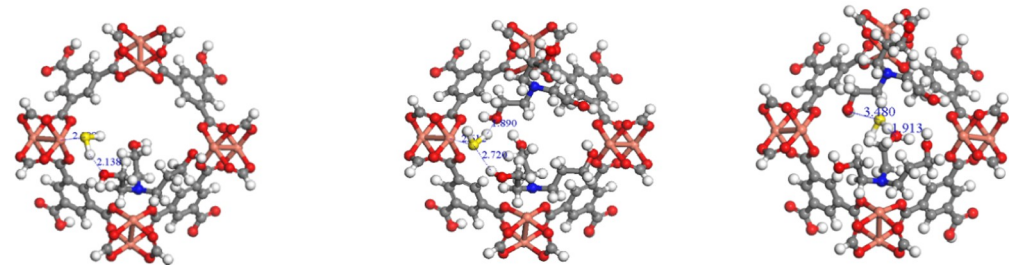

（d）E_a=67.3 kJ/mol(V-1) （e）E_a=107.7 kJ/mol(V-2) （f）E_a=79.6 kJ/mol(V-2)

Fig. 11. The models of adsorption one H_2S molecule on TEA functionalized MOF-199.

Table 4
The interaction sites and distances (Å) of each model. (The datas in red color indicate the main adsorption sites of configurations.)

	Cu-MOF	O-MOF	H-OH -TEA	O-TEA	N-TEA	C-TEA	E_a(kJ/mol)
a		3.039	2.390				87.1
b			2.561		3.240		87.3
c	2.617			1.895		3.109	92.1
d	2.588			2.138			67.3
e	2.512		2.720	1.890			107.7
f		3.480		1.913			79.6

dimethyl ethylenediamine, methyl diethanolamine and diisopropanolamine, were also used to modify MOF-199. The results were the same as MEA/MOF-199 and DEA/MOF-199. It can be concluded that both primary and secondary amines could destroy the structure of MOF-199 because of too strong interaction between the nitrogen atom in the amine and the copper in MOF-199 and therefore reduces the sulfur adsorption capacity. Rather, tertiary amine TEA modification performed quite differently result, which has a better desulfurization performance than MOF-199.

Fig. 7b presents the breakthrough curves of the TEA modified MOF-199 with different loading amount. As seen, TEA/MOF-199-1 and TEA/MOF-199-2 possess a prolonged breakthrough time and show a better desulfurization performance. The breakthrough capacity of TEA/MOF-199-2 can reach 2.74 mmol/g. However, TEA/MOF-199-3 shows a worse result with breakthrough time of 45 min and adsorption capacity of 0.33 mmol/g, which is believed to be caused by the distortion in the MOFs structure and the reduction in its surface area after overloading TEA.

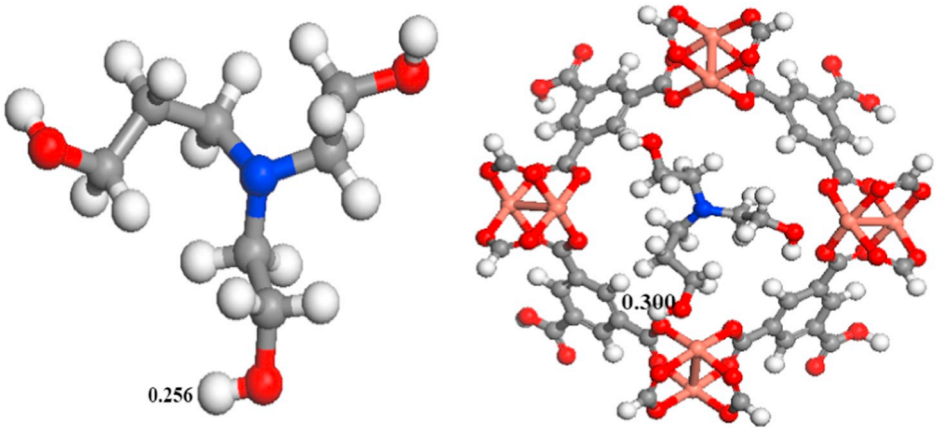

Fig. 12. Mulliken charges of hydrogen atoms in TEA hydroxyl groups before and after loading.

3.3. Investigation of H_2S-binding interactions mechanism

3.3.1. TEA load model in MOF-199

Section 2.4 has mentioned that, the square-shaped channel of MOF-199 is chosen for simulation calculation, whose diameter is 9 Å. Since the TEA molecular diameter is 7 Å, only one or two TEA molecules can be placed in the channel.

The Fig. 2 show the stable configurations for MOF-199 grafted with TEA. When one TEA molecule is placed, there are two loading models (as shown in Fig. 8a and b), where TEA are placed parallel to the channel by the interaction between oxygen atoms of TEA molecule and coppers and vertical to the channel by the interaction between nitrogen atom and copper (referred as P-1 and V-1), respectively. Fig. 8c shows the loading model (V-2) when two TEA molecules are placed vertical to the channel, in which TEA is loaded in MOF-199 through the interaction of nitrogen atoms with copper. Recording the high binding energy values of these three models, it is found that TEA can be stably grafted into the MOF-199 tunnel through the above three configurations.

3.3.2. Adsorption of H_2S on TEA functionalized MOF-199

The adsorption of H_2S on bare MOF-199 and TEA are firstly calculated, as shown in Fig. 9 and Fig. 10. It can be seen that the E_a value of H_2S on the bare MOF-199 is 54.3 kJ/mol. The E_a values on the nitrogen, hydroxyl oxygen and hydroxyl hydrogen atoms of TEA are 8.70, 17.74 and 19.72 kJ/mol, respectively.

Then the adsorption of H_2S on the TEA functionalized MOF-199 are performed and the stable adsorption configurations are obtained, as shown in Fig. 11. In addition, the interaction site and distance of H_2S on each configuration are summarized in Table 4. The first line shows the interaction sites, for example, H-OH-TEA presents the hydrogen atom of hydroxyl in TEA molecular.

Fig.11 a, b, and c show that H_2S molecular adsorbs on P-1 configuration, with E_a value of 87.1, 87.3, and 92.1 kJ/mol. In Fig. d, e, and f, H_2S adsorbs on V-1(d) and V-2(e, f), with E_a value of 67.3, 107.7, and 79.6 kJ/mol. From the comparison of binding energies of H_2S adsorption on the parent MOF-199 and TEA/MOF-199, we can find that the binding energies on TEA/MOF-199 are all larger than that on bare MOF-199.

As in the adsorption configurations of Fig. 11a and b, H_2S can interact with the hydroxyl of TEA to form an OH…S bond. In addition, H-atom of H_2S can also interact with O-atom of parent MOF-199 in Fig. 11a or the nitrogen of TEA in Fig. 11b. The above study shows that the binding energies of H_2S on the hydroxyl and nitrogen atom of TEA are 19.72 and 8.70 kJ/mol, respectively, and the previous studies have shown that the binding energy of H_2S molecule on the oxygen atoms of MOF-199 copper dimer is only 7 kJ/mol [57]. It is obvious that the binding energies of configurations Fig. 11a and b are far greater than the sum of the individual interactions. To understand why the TEA grafted MOF-199 increase the binding energies in Fig. 11a and b. We analyzed the Mulliken charges of hydrogen atoms in TEA hydroxyl groups before and after loading. The reason why this hydrogen is analyzed is because it is the main adsorption site of Fig. 11a and b, as can be seen from the interaction distances.

As show from Fig. 12, the charge of hydrogen atom of hydroxyl in TEA increases from 0.256 to 0.300 after loading to MOF-199, which indicates that the outer layer electrons of H atom is decreased. This is beneficial for hydrogen to interact with S atom which has lone pair electrons to form OH…S bond and thus Fig. 11a and b show higher binding energies.

For the Fig. 11 c, d, e and f adsorption configurations, H_2S molecule is subjected to multiple adsorption interactions, such as simultaneous interactions by the MOF-199 copper center and oxygen, hydrogen, carbon and nitrogen atoms of TEA molecule, which together contribute to the binding energies. From the interaction distances shown in Table 4, it can be seen that the interaction distances between hydroxyl oxygen of loaded TEA and H_2S are smaller than that between hydroxyl oxygen of bare TEA and H_2S (1.895, 1.890, 1.913 VS 2.218 Å), which indicates a stronger interaction happens between the hydrogen of H_2S molecule and oxygen atom of loaded TEA (expressed as O…H-HS) and results in a high binding energies (Fig. 11c, e, and f). For Fig. 11d configuration, the binding energy is 67.3 kJ/mol, lower than the configuration of c, e and f. This is thought that the interaction distance between H_2S and hydroxyl oxygen of TEA is longer (2.138 Å) and leads to a low binding energy.

4. Conclusion

To improve the performance of MOF-199 for H_2S adsorptions, modification was performed by amines impregnation. TEA was an appropriate agent for modification due to a moderate interaction with MOF-199. The H_2S working capacity of the TEA/MOF-199 at 303 K was up to 2.74 mmol/g, increased by 65% of MOF-199. Calculation by density functional theory revealed that the binding energies of H_2S adsorption on the TEA/MOF-199 were larger than that H_2S on bare MOF-199 responsible to the enhanced adsorption. The atomic properties of the loaded TEA changed compared with bare TEA and formed strong OH…S bond with H_2S. The interaction distance between O-atom of loaded TEA and H-atom of H_2S was smaller than that between bare TEA and H_2S, thus formed strong O…H-HS bond between them. In addition, our studies indicated that it is inappropriate to modify MOF-199 with primary amine and secondary amine because of the strong interaction between them.

Acknowledgment

This work was financially supported by Chinese National Science

Foundation (21878209, 21576180) and the Key Projects of National Natural Science Foundation of China (21736007).

References

[1] J. Liu, L. Cheng, S. Huang, J. Zhang, Experimental investigation of nature gas production rate's effect on the reservoirs with gas cap, J. Cle. Energy Technol. 2 (2014) 248–257.

[2] J. Liu, Y. Wei, P. Li, P. Li, Y. Zhao, R. Zhou, Selective H_2S/CO_2 separation by metal–organic frameworks based on chemical-physical adsorption, J. Phys. Chem. C 121 (2017) 13249–13255.

[3] X. Ma, X. Wang, C. Song, "Molecular basket" sorbents for separation of CO_2 and H_2S from various gas streams, J. Am. Chem. Soc. 131 (2009) 5777–5783.

[4] M. Rashtchi, G.H. Mohebali, M.M. Akbarnejad, J. Towfighi, B. Rasekh, A. Keytash, Analysis of biodesulfurization of model oil system by the bacterium, strain RIPI-22, Biochem. Eng. J. 29 (2006) 169–173.

[5] J. Fan, G. Wang, Y. Sun, C. Xu, H. Zhou, G. Zhou, J. Gao, Research on reactive adsorption desulfurization over $Ni/ZnO-SiO_2-Al_2O_3$ adsorbent in a fixed-fluidized bed reactor, Ind. Eng. Chem. Res. 49 (2010) 8450–8460.

[6] J. Liu, Y. Wang, A.I. Benin, P. Jakubczak, R.R. Willis, M.D. LeVan, CO_2/H_2O adsorption equilibrium and rates on metal–organic frameworks: HKUST-1 and Ni/DOBDC, Langmuir 26 (2010) 14301–14307.

[7] H.H. Wu, Q.H. Gong, D.H. Olson, J. Li, Commensurate adsorption of hydrocarbons and alcohols in microporous metal organic frameworks, Chem. Rev. 112 (2012) 836–868.

[8] D. Farrusseng, S. Aguado, C. Pinel, Metal–organic frameworks: opportunities for catalysis, Angew. Chem. Int. Ed. 48 (2009) 7502–7513.

[9] G. Ferey, Hybrid porous solids: past, present, future, Chem. Soc. Rev. 37 (2008) 191–214.

[10] H. Li, M. Eddaoudi, M. O'Keeffe, O.M. Yaghi, Design and synthesis of an exceptionally stable and highly porous metal-organic framework, Nature 402 (1999) 276–279.

[11] D. Britt, H. Furukawa, B. Wang, T.G. Glover, O.M. Yaghi, Highly efficient separation of carbon dioxide by a metal-organic framework replete with open metal sites, Proc. Natl. Acad. Sci. 106 (2009) 20637–20640.

[12] Z. Bao, S. Alnemrat, L. Yu, I. Vasiliev, Q. Ren, X. Lu, S. Deng, Adsorption of ethane, ethylene, propane, and propylene on a magnesiu m-based metal–organic framework, Langmuir 27 (2011) 13554–13562.

[13] H. Wu, W. Zhou, T. Yildirim, High-capacity methane storage in metal–organic frameworks M2(dhtp): the important role of open metal sites, J. Am. Chem. Soc. 131 (2009) 4995–5000.

[14] X. Zhou, Y. Zhang, X. Yang, L. Zhao, G. Wang, Functionalized IRMOF-3 as efficient heterogeneous catalyst for the synthesis of cyclic carbonates, J. Mol. Catal. A Chem. 361 (2012) 12–16.

[15] B. Supronowicz, A. Mavrandonakis, T. Heine, Interaction of small gases with the unsaturated metal centers of the HKUST-1 metal organic framework, J. Phys. Chem. C 117 (2013) 14570–14578.

[16] B. Levasseur, C. Petit, T.J. Bandosz, Reactive adsorption of NO_2 on copper-based metal–organic framework and graphite oxide/metal–organic framework composites, ACS Appl. Mater. Inter. 2 (2010) 3606–3613.

[17] L. Hamon, C. Serre, T. Devic, T. Loiseau, F. Millange, G. Férey, G. De Weireld, Comparative study of hydrogen sulfide adsorption in the MIL-53 (Al, Cr, Fe), MIL-47 (V), MIL-100 (Cr), and MIL-101 (Cr) metal-organic frameworks at room temperature, J. Am. Chem. Soc. 131 (2009) 8775–8777.

[18] Y. Li, L.J. Wang, H.L. Fan, J. Shangguan, H. Wang, J. Mi, Removal of sulfur compounds by a copper-based metal organic framework under ambient conditions, Energy Fuel 29 (2014) 298–304.

[19] Y. Li, W. Jiang, P. Tan, X. Liu, D. Zhang, L. Sun, What matters to the adsorptive desulfurization performance of metal-organic frameworks? J. Phys. Chem. C 119 (2015) 21969–21977.

[20] G. Blanco-Brieva, J.M. Campos-Martin, S.M. Al-Zahrani, J.L.G. Fierro, Effectiveness of metal-organic frameworks for removal of refractory organo-sulfur compound present in liquid fuels, Fuel 90 (2011) 190–197.

[21] S. Achmann, G. Hagen, M. Hämmerle, I.M. Malkowsky, C. Kiener, R. Moos, Sulfur removal from low-sulfur gasoline and diesel fuel by metal-organic frameworks, Chem. Eng. Technol. 33 (2010) 275–280.

[22] L. Hamon, H. Leclerc, A. Ghoufi, L. Oliviero, A. Travert, J.C. Lavalley, T. Devic, C. Serre, G. Férey, G. De Weireld, A. Vimont, G. Maurin, Molecular insight into the adsorption of H_2S in the flexible MIL-53 (Cr) and rigid MIL-47 (V) MOFs:infrared spectroscopy combined to molecular simulations, J. Phys. Chem. C 115 (2011) 2047–2056.

[23] Y. Shiraishi, K. Tachibana, T. Hirai, I. Komasawa, Desulfurization and denitrogenation process for light oils based on chemical oxidation followed by liquid–liquid extraction, Ind. Eng. Chem. Res. 41 (2002) 4362–4375.

[24] H. Demir, K.S. Walton, D.S. Sholl, Computational screening of functionalized UiO-66 materials for selective contaminant removal from air, J. Phys. Chem. C 121 (2017).

[25] J.N. Joshi, G. Zhu, J.J. Lee, E.A. Carter, C.W. Jones, R.P. Lively, K.S. Walton, Probing metal–organic framework design for adsorptive natural gas purification, Langmuir 34 (2018) 8443–8450.

[26] X.L. Wang, H.L. Fan, Z. Tian, E.Y. He, Y. Li, J. Shangguana, Adsorptive removal of sulfur compounds using IRMOF-3 at ambient temperature, Appl. Surf. Sci. 289 (2014) 107–113.

[27] S.M. Cohen, Postsynthetic methods for the functionalization of metal–organic frameworks, Chem. Rev. 112 (2012) 970–1000.

[28] S.J. Garibay, Z.Q. Wang, K.K. Tanabe, S.M. Cohen, Postsynthetic modification: a versatile approach toward multifunctional metal-organic frameworks, Inorg. Chem. 48 (2009) 7341–7349.

[29] B. Zheng, J. Bai, J. Duan, L. Wojtas, M.J. Zaworotko, Enhanced CO_2 binding affinity of a high-uptake rht-type metal-organic framework decorated with acylamide groups, J. Am. Chem. Soc. 133 (2010) 748–751.

[30] Y. Luan, Y. Qi, H. Gao, R.S. Andriamitantsoa, N. Zheng, G. Wang, A general post-synthetic modification approach of amino-tagged metal–organic frameworks to access efficient catalysts for the Knoevenagel condensation reaction, J. Mater. Chem. A 3 (2015) 17320–17331.

[31] G. Arom'ı, L.A. Barrios, O. Roubeau, P. Gamez, Triazoles and tetrazoles: prime ligands to generate remarkable coordination materials, Chem. Rev. 255 (2011) 485–546.

[32] S. Hasegawa, S. Horike, R. Matsuda, S. Furukawa, K. Mochizuki, Y. Kinoshita, S. Kitagawa, Three-dimensional porous coordination polymer functionalized with amide groups based on tridentate ligand: selective sorption and catalysis, J. Am. Chem. Soc. 129 (2007) 2607–2614.

[33] A. Modak, J. Mondal, A. Bhaumik, Porphyrin based porous organic polymer as bifunctional catalyst for selective oxidation and Knoevenagel condensation reactions, Appl. Catal. A 459 (2013) 41–51.

[34] L.T.L. Nguyen, K.K.A. Le, H.X. Truong, N.T.S. Phan, Metal–organic frameworks for catalysis: the Knoevenagel reaction using zeolite imidazolate framework ZIF-9 as an efficient heterogeneous catalyst, Catal. Sci. Technol. 2 (2012) 521–528.

[35] J.A. Mason, T.M. McDonald, T.-H. Bae, J.E. Bachman, K. Sumida, J.J. Dutton, S.S. Kaye, J.R.J. Long, Application of a high-throughput analyzer in evaluating solid adsorbents for post-combustion carbon capture via multicomponent adsorption of CO_2, N_2, and H_2O, J. Am. Chem. Soc. 137 (2015) 4787–4803.

[36] P.J. Milner, R.L. Siegelman, A.C. Forse, M.I. Gonzalez, T. Runčevski, J.D. Martell, J.A. Reimer, J.R. Long, A diaminopropane-appended metal–organic framework enabling efficient CO_2 capture from coal flue gas via a mixed adsorption mechanism, J. Am. Chem. Soc. 139 (2017) 13541–13553.

[37] R.L. Siegelman, T.M. McDonald, M.I. Gonzalez, J.D. Martell, P.J. Milner, J.A. Mason, A.H. Berger, A.S. Bhown, J.R. Long, Controlling cooperative CO_2 adsorption in diamine-appended Mg_2(dobpdc) metal–organic frameworks[J], J. Am. Chem. Soc. 139 (2017) 10526–10538.

[38] S. Xian, F. Chen, M. Wu, Q. Xia, H. Wang, Z. Li, Vapor-enhanced CO_2 adsorption mechanism of composite PEI@ZIF-8 modified by polyethyleneimine for CO_2/N_2 separation, Chem. Eng. J. 280 (2015) 363–369.

[39] S. Choi, T. Watanabe, T. Bae, D.S. Sholl, C.W. Jones, Modification of the mg/DOBDC MOF with amines to enhance CO_2 adsorption from ultradilute gases, J. Phys. Chem. Lett. 3 (2012) 1136–1141.

[40] X. Su, L. Bromberg, V. Martis, F. Simeon, A. Huq, T.A. Hatton, Postsynthetic functionalization of Mg-MOF-74 with tetraethylenepentamine: structural characterization and enhanced CO_2 adsorption, ACS Appl. Mater. Inter. 9 (2017) 11299–11306.

[41] Y. Peng, H. Huang, Y. Zhang, C. Kang, S. Chen, L. Song, D. Liu, C. Zhong, A versatile MOF-based trap for heavy metal ion capture and dispersion, Nat. Commun. 9 (2018) 187.

[42] B. Li, X. Dong, H. Wang, D. Ma, K. Tan, S. Jensen, B.J. Deibert, J. Butler, J. Cure, Z. Shi, T. Thonhauser, Y.J. Chabal, Y. Han, J. Li, Capture of organic iodides from nuclear waste by metal-organic framework-based molecular traps, Nat. Commun. 8 (2017) 485.

[43] B. Levasseur, C. Petit, T.J. Bandosz, Reactive adsorption of NO_2 on copper-based metal-organic framework and graphite oxide/metal-organic framework composites, ACS Appl. Mater. Inter. 2 (2010) 3606–3613.

[44] K. Schlichte, T. Kratzke, S. Kaskel, Improved synthesis, thermal stability and catalytic properties of the metal-organic framework compound $Cu_3(BTC)_2$, Microporous Mesoporous Mater. 73 (2004) 81–88.

[45] B. Supronowicz, A. Mavrandonakis, T. Heine, Interaction of small gases with the unsaturated metal centers of the HKUST-1 metal organic framework, J. Phys. Chem. C 117 (2013) 14570–14578.

[46] K. Schlichte, T. Kratzke, S. Kaskel, Improved synthesis, thermal stability and catalytic properties of the metal-organic framework compound $Cu_3(BTC)_2$, Microporous Mesoporous Mater. 73 (2004) 81–88.

[47] L. Hamon, E. Jolimaître, G.D. Pringruber, CO_2 and CH_4 separation by adsorption using cu-BTC metal-organic framework, Ind. Eng. Chem. Res. 49 (2010) 7497–7503.

[48] Z. Chen, L. Ling, B. Wang, H. Fan, J. Shangguan, J. Mi, Adsorptive desulfurization with metal-organic frameworks: a density functional theory investigation, Appl. Sur. Sci. 387 (2016) 483–490.

[49] B. Delley, From molecules to solids with the DMol3 approach, J. Chem. Phys. 113 (2000) 7756–7764.

[50] D. Sholl, J.A. Steckel, Density Functional Theory: A Practical Introduction, Wiley, 2011.

[51] B. Delley, Hardness conserving semilocal pseudopotentials, Phys. Rev. B 66 (2002) 155125.

[52] S. Vairam, S. Govindarajan, New hydrazinium salts of benzene tricarboxylic and tetracarboxylic acids—preparation and their thermal studies, Thermochim. Acta 414 (2004) 263–270.

[53] E. Biemmi, T. Bein, N. Stock, Synthesis and characterization of a new metal organic framework structure with a 2D porous system:$(H_2NEt_2)_2[Zn_3(BDC)_4]\cdot 3DEF$, Solid State Sci. 8 (2006) 363–370.

[54] Z.-Q. Bai, L.-Y. Yuan, L. Zhu, Z.-R. Liu, S.-Q. Chu, L.-R. Zheng, J. Zhang, Z.-F. Chai, W.-Q. Shi, Introduction of amino groups into acid-resistant MOFs for enhanced U (VI) sorption, J. Mater. Chem. A 3 (2015) 525–534.

[55] G.W. Peterson, G.W. Wagner, A. Balboa, J. Mahle, T. Sewell, C.J. Karwacki, Ammonia vapor removal by $Cu_3(BTC)_2$ and its characterization by MAS NMR, J. Phys. Chem. C 113 (2009) 13906–13917.
[56] R.S. Kumar, S.S. Kumar, M.A. Kulandainathan, Efficient electrosynthesis of highly active $Cu_3(BTC)_2$-MOF and its catalytic application to chemical reduction, Microporous Mesoporous Mater. 168 (2013) 57–64.
[57] H. Zhang, Z. Zhang, C. Yang, L. Ling, B. Wang, H. Fan, A computational study of the adsorptive removal of H_2S by MOF-199, J. Inorg. Organomet. P. 28 (2018) 694–701.